

# Propagators and Dimensional Reduction of Hot SU(2) Gauge Theory

A. Cucchieri

*IFSC-USP, Caixa Postal 369, 13560-970 Sao Carlos, SP, Brazil*

F. Karsch and P. Petreczky

*Fakultät für Physik, Universität Bielefeld,*

*P.O. Box 100131, D-33501 Bielefeld, Germany*

(October 26, 2018)

We investigate the large distance behavior of the electric and magnetic propagators of hot SU(2) gauge theory in different gauges using lattice simulations of the full 4d theory and the effective, dimensionally reduced 3d theory. Comparison of the 3d and 4d propagators suggests that dimensional reduction works surprisingly well down to the temperature  $T = 2T_c$ . Within statistical uncertainty the electric screening mass is found to be gauge independent. The magnetic propagator, on the other hand, exhibits a complicated gauge dependent structure at low momentum.

## I. INTRODUCTION

Understanding the large distance behavior of the static electric and magnetic propagators in hot SU(N) gauge theory is of interest for several reasons. First of all it is related to the screening phenomenon in a hot non-Abelian plasma. In fact, the concepts of electric and magnetic masses extracted from these propagators form to a large extent the basis for our intuitive understanding of screening in non-abelian gauge theories [1]. Furthermore, the concept of screened electric propagators finds application in refined perturbative calculations (hard thermal loop resummation) [2–4]. Non-perturbative calculations of these propagators thus can provide a bridge between perturbative and non-perturbative descriptions of the electric screening phenomenon.

Of course, a draw back of such an approach is that the gluon propagator itself is a gauge dependent quantity. One thus has to question to what extent the results extracted from these propagators have a physical meaning. The poles of the gluon propagator at finite temperature were proven to be gauge invariant in perturbation theory [5]. However, for static quantities like the Debye mass static magnetic fields can lead to a breakdown of perturbation theory. The Debye mass cannot be defined perturbatively beyond leading order [6,7]. Non-perturbatively the problem of gauge independence of the screening masses thus is an open question.

It has been shown that at high temperature the large distance behavior of a SU(N) gauge theory can be described in terms of the dimensionally reduced effective theory, i.e. the three dimensional adjoint Higgs model [8–15]. The screening masses extracted from gauge invariant correlators were studied in terms of the effective three dimensional (3d) theory [12–17] and were compared with the corresponding results from four dimensional (4d) simulations [18,19]. The relation between the propagator masses and the masses extracted from gauge invariant correlators was discussed in [8]. The screening masses extracted from gauge invariant correlators correspond to masses of some bound states of the 3d effective theory and are several times larger than masses extracted from propagators.

In the present paper we extend our earlier studies on the electric and magnetic propagators [8,20,21]. Contrary to Refs. [8,20,21] where propagators were studied only in Landau gauge we consider here a class of generalized Landau gauges, the Coulomb gauge, the maximally Abelian gauge and the static time averaged Landau gauge. We study the propagators in terms of the 3d effective theory as well as in the 4d theory at finite temperature. A comparison of the propagators in the full 4d and in the 3d effective theory provides further evidence for the applicability of dimensional reduction. A detailed study of finite size effects in the propagators shows that the picture of magnetic screening given in Refs. [8,20,21] needs to be revised to some extent. First results from our analysis of the magnetic sector have been presented in Ref. [22].

The paper is organized as follows. In section II we discuss questions related to gauge fixing and the definition of propagators in finite temperature SU(2) theory as well as in the dimensionally reduced effective theory, the 3d adjoint Higgs model. Section III contains our main results on electric and magnetic propagators and the analysis of their gauge and volume dependence. Finally we give our conclusion in section IV. In an Appendix details of the determination of the parameters of the effective theory are discussed.

## II. GLUON PROPAGATORS IN FINITE TEMPERATURE SU(2) GAUGE THEORY

In this section we define the actions we use for our simulations in three and four dimensions and introduce our basic notation for gauge fields, gluon propagators and the different gauges we have analyzed.

### A. Actions in three and four dimensions

In four dimensions (4d) all our calculations are performed with the standard Wilson action for SU(2) lattice gauge theory,

$$S_W = \beta_4 \sum_{x, \nu > \mu} \left[ 1 - \frac{1}{2} \text{Tr} U_\mu(x) U_\nu(x + \hat{\mu}) U_\mu^\dagger(x + \hat{\nu}) U_\nu^\dagger(x) \right], \quad (1)$$

where  $U_\mu(x) \in SU(2)$  are the usual link variables and  $\beta_4 = 4/g_4^2$ . In three dimensions (3d) the standard dimensional reduction process leads us to consider the 3d adjoint Higgs model

$$S = -\beta_3 \sum_{\mathbf{x}, \nu > \mu} \frac{1}{2} \text{Tr} U_\mu(\mathbf{x}) U_\nu(\mathbf{x} + \hat{\mu}) U_\mu^\dagger(\mathbf{x} + \hat{\nu}) U_\nu^\dagger(\mathbf{x}) - \beta_3 \sum_{\mathbf{x}, \hat{\mu}} \frac{1}{2} \text{Tr} A_0(\mathbf{x}) U_\mu(\mathbf{x}) A_0(\mathbf{x} + \hat{\mu}) U_\mu^\dagger(\mathbf{x}) \\ + \beta_3 \sum_{\mathbf{x}} \left[ \left( 3 + \frac{1}{2} h \right) \frac{1}{2} \text{Tr} A_0^2(\mathbf{x}) + x \left( \frac{1}{2} \text{Tr} A_0^2(\mathbf{x}) \right)^2 \right], \quad (2)$$

where  $\beta_3$  now is related to the dimensionful 3d gauge coupling and the lattice spacing  $a$ , *i.e.*  $\beta_3 = 4/g_3^2 a$ . The adjoint Higgs field is parameterized by hermitian matrices  $A_0 = \sum_a \sigma^a A_0^a$  ( $\sigma^a$  are the usual Pauli matrices) [12]. Furthermore,  $x$  parameterizes the quartic self coupling of the Higgs field and  $h$  denotes the bare Higgs mass squared. The relation between the 3d and the 4d couplings will be discussed in an Appendix. We also note that the indices  $\mu, \nu$ , of course, run from 0 to 3 in four dimensions and from 1 to 3 in three dimensions. Although we will not always mention this difference explicitly it should be obvious from the context how various sums that appear have to be interpreted.

### B. Gauge fixing

As we want to analyze properties of the gluon propagator, which is a gauge dependent quantity, we have to fix a gauge on each configuration on which we want to calculate this observable. In the past most studies of the gluon propagator have been performed in Landau gauge. Here we will consider a class of  $\lambda$ -gauges which are generalizations of gauges that have been introduced in [23,24] to smoothly interpolate between Landau and Coulomb gauge. In the continuum these gauges correspond to the gauge condition

$$\sum_{\mu} \lambda_{\mu} \partial_{\mu} A_{\mu} = 0 \quad . \quad (3)$$

On the lattice these gauges are realized by maximizing the quantity

$$\text{Tr} \sum_{\mu, x} \lambda_{\mu} U_{\mu}(x) \quad . \quad (4)$$

In 4d the Landau gauge condition thus corresponds to the case  $\lambda_{\mu} \equiv 1$  for all  $\mu = 0, \dots, 3$ , while the Coulomb gauge is given by  $\lambda_0 = 0$  and  $\lambda_i = 1$  for  $i = 1, 2, 3$ . In the latter case we have to impose an additional gauge condition for the residual gauge degree of freedom. We do this by demanding

$$\sum_{\mathbf{x}} U_0(x_0, \mathbf{x}) = u_0 \quad , \quad (5)$$

to be independent of  $x_0$ . In addition to the  $\lambda$ -gauges we also consider the Maximally Abelian gauge (MAG) which can be realized by maximizing the quantity [25]

$$\sum_{x,\mu} \text{Tr} [\sigma_3 U_\mu(x) \sigma_3 U_\mu^\dagger(x)] \quad , \quad (6)$$

with  $\sigma_3$  being a Pauli matrix. Also in this case one has to fix a residual gauge degree of freedom which we do by imposing a U(1)-Landau gauge condition [26]. In 4d SU(2) gauge theory we also consider the static time-averaged Landau gauge (STALG) introduced in [27,28]. In the continuum it is defined by

$$\partial_0 A_0(x_0, \mathbf{x}) = 0, \quad \sum_{x_0} \sum_{i=1}^3 \partial_i A_i = 0. \quad (7)$$

On lattice this gauge is realized in two steps. First we maximize the quantity  $\text{Tr} \sum_x U_0(x)$ . In the second step we maximize the quantity

$$\text{Tr} \sum_{i=1}^3 \sum_x U_i(x) \quad (8)$$

performing  $x_0$ -independent gauge transformations.

While the notion of Landau and Maximally Abelian gauges carries over easily to the 3d case we have to explain a bit more in detail our notion of  $\lambda$ -gauges in 3d. We have considered two versions of  $\lambda$ -gauge:

$$\lambda_3\text{-gauge} : \quad \partial_1 A_1 + \partial_2 A_2 + \lambda_3 \partial_3 A_3 = 0 \quad (9)$$

$$\lambda_1\text{-gauge} : \quad \lambda_1 \partial_1 A_1 + \partial_2 A_2 + \partial_3 A_3 = 0 \quad (10)$$

The  $\lambda_1$ -gauges are more closely related to the 4d  $\lambda$ -gauges considered by us; in both cases the rotational symmetry of the gauge condition is broken in a direction orthogonal to the  $x_3$  (or  $z$ ) direction which we are going to use for separating the sources in our correlation functions. Furthermore, we introduce in 3d the so-called Coulomb gauges ( $c_1$  gauges) which fix the gauge in a plane transverse to the  $z$ -direction,

$$c_1\text{-gauge} : \quad c_1 \partial_1 A_1 + \partial_2 A_2 = 0 \quad . \quad (11)$$

Of course, as in the 4d case we again need an additional gauge condition for the residual gauge degree of freedom. The case  $c_1 = 1.0$  is the usual Coulomb gauge. This gauge has the advantage that a positive definite transfer matrix exists in the  $z$ -direction.

In our numerical calculations the gauge fixing was performed using a standard iterative algorithm accelerated by an overrelaxation step [29] as well as by using a stochastic overrelaxation algorithm [30].

When analyzing observables in a fixed gauge one also has to address the question to what extent Gribov copies can influence the result. This problem will not be discussed here. It previously has been studied in 4d SU(2) gauge theories at zero temperature [31] as well as at non-zero temperature [20]. In both cases no influence of Gribov copies on the gluon propagators was found within the statistical accuracy achieved in these studies.

### C. Gauge fields and gluon propagators

Definitions of the lattice gauge field  $A_\mu(x)$  utilize the naive continuum relation between the lattice link variables  $U_\mu(x)$  and the gauge field variables in the continuum limit, *i.e.*  $U_\mu(x) = \exp(igaA_\mu(x))$ . A straightforward definition thus is

$$A_\mu(x) = \frac{1}{2iga} [U_\mu(x) - U_\mu^\dagger(x)] \quad , \quad (12)$$

which in the continuum limit differs from the continuum gauge fields by  $\mathcal{O}((ag)^2)$  corrections. Here  $a$  is the lattice spacing and  $g$  either the 3d or 4d bare gauge coupling. Other possible definitions for  $A_\mu(x)$  which formally lead to smaller discretization errors were considered in [32]. It was found there that up to an overall multiplicative constant the difference in magnetic and electric propagators due to different definitions of the gauge field is much smaller than the statistical errors. We note that the definition (12) of the gauge field assumes that the link variable  $U_\mu$  is close to the unit matrix. This seems to be the case for all gauges considered except the Coulomb gauge. In the case of Coulomb gauge the gauge fixing procedure does not force the temporal link to be close to the unit matrix. Only the spatial links turn out to be close to the unit matrix. For instance, for links averaged over a lattice volume of size  $12^2 \times 24 \times 4$  we find for  $\beta_4 = 2.512$  (corresponding to  $2T_c$ )  $\langle \text{Tr}U_0/2 \rangle = 0.576(4)$  and  $\langle \text{Tr}U_i/2 \rangle = 0.90089(6)$ . These numbers should be compared with the corresponding ones in Landau gauge:  $\langle \text{Tr}U_0/2 \rangle = 0.8879(1)$  and  $\langle \text{Tr}U_i/2 \rangle = 0.88709(7)$ . One can expect that  $\text{Tr}U_0/2$  gets closer to 1 as one approaches the continuum limit. Indeed for the Coulomb gauge on a  $24^2 \times 48 \times 8$  lattice at  $\beta = 2.74$  (also corresponding to  $2T_c$ ) we find  $\langle \text{Tr}U_0/2 \rangle = 0.625(6)$ . However, from these numbers it is clear that very large values of  $N_\tau$ , i.e. large couplings  $\beta_4$ , are necessary to get a meaningful definition of the  $A_0$  field. Therefore we will use the 4d Coulomb gauge only to analyze magnetic propagators.

The lattice gluon propagators in d-dimension are defined as

$$D_{\mu\mu}(z) = \frac{1}{a^d \Omega} \left\langle a \sum_{x_3, b} Q_\mu^b(x_3 + z) Q_\mu^b(x_3) \right\rangle. \quad (13)$$

Here  $Q_\mu^b(x_3)$  is a sum over all gauge fields in a hyperplane orthogonal to  $x_3$ ,

$$Q_\mu^b(x_3) = a^{d-1} \sum_{x_\perp} A_\mu^b(x_\perp, x_3), \quad (14)$$

with  $A_\mu^b(x) = \frac{1}{2} \text{Tr}[A_\mu(x) \sigma^b]$ ;  $x_\perp = (x_1, x_2)$  in 3d and  $x_\perp = (x_0, x_1, x_2)$  in 4d, respectively. Furthermore,  $\Omega = N^2 N_z$  is the lattice volume in 3d and  $\Omega = N^2 N_z N_t$  in 4d<sup>1</sup>. The electric and magnetic propagators are then defined in the usual way (see e.g. Refs. [20,21]),

$$D_E(z) = D_{00}(z) \quad , \quad D_M(z) = \frac{1}{2} (D_{11}(z) + D_{22}(z)) \quad . \quad (15)$$

$D_{33}(z)$  is not included in the definition of  $D_M(z)$  because it is constant in  $\lambda$  and Coulomb gauges. We will also consider momentum space propagators which are obtained through a one dimensional Fourier transformation,

$$\tilde{D}_{\mu\mu}(k) = a \sum_{z=0}^{N_z-1} e^{ikz} D_{\mu\mu}(z), \text{ with } k = \frac{2\pi n}{N_z}, n = 0, 1, \dots, N_z/2 \quad (16)$$

We use the standard definition for the momentum space magnetic propagator (see e.g. [33,34])

$$\tilde{D}_M(k) = \frac{1}{3} \sum_{\mu=1}^3 D_{\mu\mu}(k). \quad (17)$$

We note that we include here  $\tilde{D}_{33}$  in the definition of the momentum space propagators in order to take into account the contribution of the constant component  $D_{33}(z)$ , which only influences the zero mode contribution  $\tilde{D}_{\mu\mu}(k=0)$ . The electric propagator in momentum space is simply defined by  $\tilde{D}_E(k) = \tilde{D}_{00}(k)$ . In order to absorb additional cut-off effects in momentum space propagators we find it useful to analyze these in terms of the momenta  $p \equiv |2 \sin(k/2)|$  rather than the lattice momenta  $k$ . In the following we thus will use  $p$  instead of  $k$  as a definition for our lattice momenta. For the analysis of the long distance behavior of these correlation functions it is customary and, in fact, quite instructive to consider *local masses*, which are defined by

$$\frac{D_i(z)}{D_i(z+1)} = \frac{\cosh(m_i(z)(z - N_z/2))}{\cosh(m_i(z)(z + 1 - N_z/2))}, \quad (18)$$

---

<sup>1</sup>We will also use the notation  $V = N^2 N_z$  for the spatial volume in 3d and 4d.

with  $i = E, M$ . If the propagators decay exponentially starting from some value of  $z$ , the corresponding local masses will reach a plateau.

All our 4d simulations have been performed at a temperature  $T = 2T_c$ . The values for the 4d coupling  $\beta_4$  corresponding to this temperature were taken from Ref. [21] and are given in Table I together with the corresponding lattice volumes used in our 4d simulations.

$\beta_4 = 2.512$	$8^2 \times 16 \times 4$
	$12^2 \times 24 \times 4$
	$16^2 \times 32 \times 4$
	$20^2 \times 40 \times 4$
	$24^2 \times 48 \times 4$
	$28^2 \times 56 \times 4$
$\beta_4 = 2.740$	$32^2 \times 64 \times 4$
	$16^2 \times 32 \times 8$
	$24^2 \times 48 \times 8$

TABLE I. Couplings and lattice volumes used in the 4d simulations of finite temperature SU(2) gauge theory.

We give the choice of parameters for our 3d simulations in the next subsection. The cutoff dependence is discussed for the magnetic and electric propagators separately in section III.

#### D. 3d versus 4d calculations

Most of the results we are going to discuss in the following section have been obtained through simulations in the dimensionally reduced version of the 4d SU(2) gauge theory at finite temperature. As we do want to compare our results obtained in 3d with corresponding results in the 4d theory obtained at a temperature  $T = 2T_c$  we should check that dimensional reduction yields reliable results at temperatures this close to the critical point. In Refs. [13–15] it was shown that the effective theory is capable to describe the long distance behavior of some gauge invariant correlators in SU(2) and SU(3) gauge theories at these temperatures. A similar conclusion has been reached for the 2d dimensionally reduced version of the 3d SU(3) gauge theory at finite temperature [35].

We have performed a detailed analysis of propagators calculated in Landau gauge in 4d and 3d at  $T = 2T_c$ . The latter has been simulated at values of  $h$  corresponding to the metastable region of the 3d adjoint Higgs model, *i.e.* for  $\beta = 11$ ,  $h = -0.3773$  and  $x = 0.099$  (see appendix for details). The 4d simulations have been performed at  $\beta = 2.74$  on lattices given in Table I. In order to compare the propagators obtained from simulations in 3d and 4d we have normalized them to unity at distance  $zT = 0$ . The results are shown in Figure 1. As one can see from the figure the 3d and 4d results for the electric as well as for the magnetic propagators are in excellent agreement. It is interesting to note that good agreement between 3d and 4d propagators is found already at relatively short distances, although the 3d effective theory is expected to describe the 4d physics only at distance  $zT > 1$ . The above result implies that dimensional reduction works quite well even at  $T = 2T_c$  and can be established by comparing gauge fixed observables. In Figure 2 we compare the electric and magnetic propagators calculated from full 4d and effective 3d theories at  $2T_c$  for the maximally Abelian gauge. As one can see from the figure a good agreement between 4d and 3d results exists also here, although it is a priori not clear in which sense the 3d Maximally Abelian gauge corresponds to the 4d Maximally Abelian gauge. The agreement between the magnetic propagators in Figure 2 shows that the two gauges are quite similar. A possible reason for this agreement is the decoupling of the  $A_0$  field from the dynamics of spatial (magnetic) gauge fields which will be discussed in the next section. We note, however, already here that the magnetic propagators calculated in Landau and Maximally Abelian gauges, respectively, show quite a different long distance behavior. This is evident from the comparison of Figure 1 and Figure 2 and will be analyzed in much more detail in the next section. Also the apparent volume dependence visible in these figures will be discussed later in more detail.

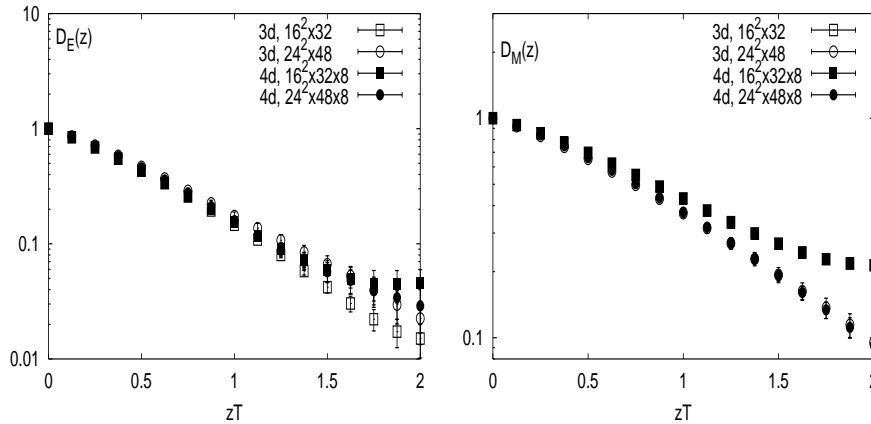


FIG. 1. Comparison of 4d and 3d data for the electric (left) and magnetic (right) gluon propagator in Landau gauge calculated at  $T = 2T_c$ .

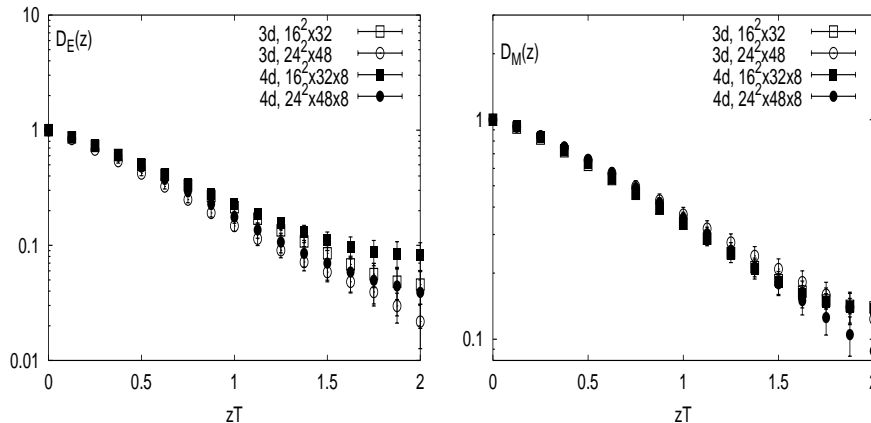


FIG. 2. Comparison of 4d and 3d data for the electric (left) and magnetic (right) gluon propagator in Maximally Abelian gauge calculated at  $T = 2T_c$ .

### III. NUMERICAL RESULTS ON ELECTRIC AND MAGNETIC GLUON PROPAGATORS

In this section we will discuss our numerical results obtained from simulations in three and four dimensions. The main purpose of this investigation was to quantify the gauge dependence of the electric and magnetic gluon propagators and analyze to what extent gauge invariant masses can be extracted from the long distance behavior of the gluon correlation functions.

In Figure 3 we show results from a calculation of the magnetic propagator in 4d finite temperature gauge theory in different  $\lambda$ -gauges including the Coulomb gauge limit. All the  $\lambda$ -gauges yield identical magnetic propagators. In fact, one should expect that all  $\lambda$ -gauges do lead to identical propagators on an infinite spatial lattice. For static configurations ( $\partial_0 A_0 = 0$ ) the gauge condition for the  $\lambda$ -gauges,  $\lambda \partial_0 A_0 + \partial_i A_i = 0$  is up to multiplicative factors identical to the 3d Landau gauge condition. As we have shown that the 4d propagators in Landau gauge can be mapped onto the 3d propagators this has to be the case also for the 4d propagators calculated in  $\lambda$ -gauges. The same holds for STALG.

We also note, that magnetic propagators show strong volume dependence at distances  $zT \gtrsim 1$ . This effect may be traced back to the influence of zero mode contributions to the propagators [45] which are different in different gauges and give a volume dependent positive contribution to the correlation functions. Zero mode contributions are most prominent in the long distance behavior of the correlation functions calculated on finite lattices.

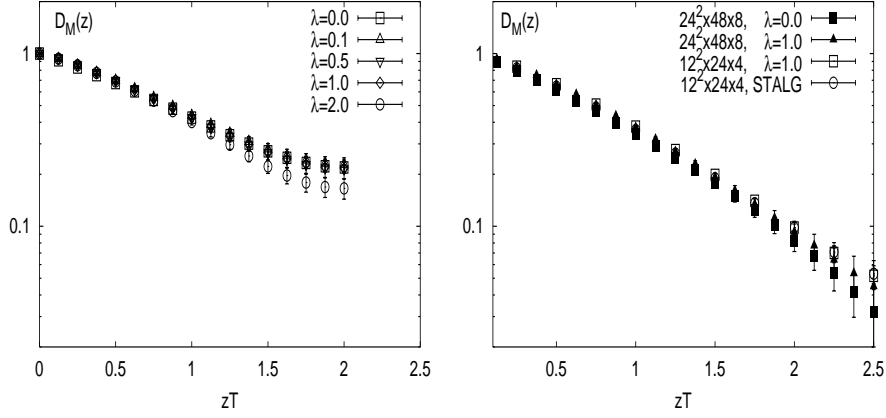


FIG. 3. The magnetic propagator in  $\lambda$  gauges on a  $16^2 \times 32 \times 8$  lattice (left), as well as on  $24^2 \times 48 \times 8$  and  $12^2 \times 24 \times 4$  lattices (right) at  $T = 2T_c$ . Here also the propagator in STALG is shown. The propagators were normalized to 1 at  $z = 0$ .

In Figure 4 we summarize our results for electric propagators. As in the case of magnetic propagators, electric propagators calculated in different 4d  $\lambda$ -gauges as well as in STALG agree with each other as expected. Contrary to magnetic propagators the electric propagators show no significant volume dependence. We also note that the cut-off effects seem to be small both for electric and magnetic propagators (cf. Figures 3 and 4). The issues of volume and cut-off dependence will be discussed separately for electric and magnetic propagators in the following two subsections.

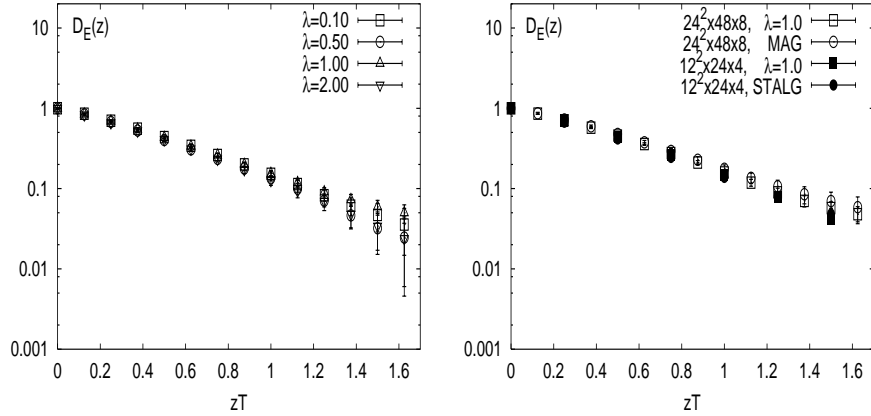


FIG. 4. The electric propagators in different gauges. Shown is the electric propagator measured on  $16^2 \times 32 \times 8$  (left) and on  $24^2 \times 48 \times 8$  and  $12^2 \times 24 \times 4$  (right). The propagators were normalized to 1 at  $z = 0$ .

### A. The magnetic gluon propagator

In this section we will discuss in more detail our results on magnetic propagators. Previous lattice calculations of the magnetic propagators in hot SU(2) gauge theory in 4d [21] and 3d [8] gave evidence for its exponential decay in coordinate space and thus indicated the existence of a magnetic mass. A non-zero magnetic mass was also found in analytical approaches based on gap equation [37–39] and a non-perturbative analysis of 2+1 dimensional gauge theory [40]. Nonetheless, it has been questioned whether a magnetic mass in non-abelian gauge theories does exist [41,42]. In Ref. [33] the Landau gauge propagators of 3d pure gauge theory were studied on fairly large lattices and were found to be infrared suppressed<sup>2</sup>. Such a behavior clearly is in conflict with the existence of a simple pole mass. In order

<sup>2</sup>Similar results were found in 4d SU(N) gauge theory at zero temperature [43,44].

to further investigate this problem simulations on larger lattices are needed to explore the long distance regime of the correlation functions. This can be achieved in the 3d reduced theory which gives a good description of the 4d theory even at temperatures a few times  $T_c$ . We thus concentrate, in the following on a discussion of results obtained from our calculations in 3d. In fact, it also has been observed already in earlier calculations that the magnetic propagators of the 3d adjoint Higgs model are very close to the corresponding propagators of 3d pure gauge theory. We thus further restrict our analysis of the magnetic propagators to the limit of 3d pure gauge theory. Where appropriate we will perform a comparison with results obtained from the 3d adjoint Higgs model and the 4d SU(2) gauge theory.

In order to get control over the propagators also in the continuum as well as in the infinite volume limit we have performed calculations for  $\beta_3 = 5, 5.5, 6, 8$  and  $16$  on different lattice volumes. The simulation parameters are summarized in Table II.

$\beta_3 = 5$	$\beta_3 = 5.5$	$\beta_3 = 6$	$\beta_3 = 8$	$\beta_3 = 16$
$10^2 \times 20$	$16^2 \times 32$	$72^3$	$16^2 \times 32$	$32^2 \times 64$
$16^3$	$24^2 \times 48$		$24^2 \times 48$	$40^2 \times 96$
$24^3$			$28^2 \times 56$	$48^2 \times 96$
$30^3$			$32^3$	$64^3$
$32^3$			$32^2 \times 64$	$96^3$
$40^3$			$48^3$	
$48^3$			$48^2 \times 64$	
$56^3$			$64^3$	
$60^3$			$96^3$	
$64^3$				
$72^3$				
$96^3$				

TABLE II: Lattice volumes used at different values of  $\beta_3$  in our 3d calculations of the magnetic gluon propagator.

It has been pointed out in [45] that zero modes can give sizeable contributions to gluon correlation functions. In terms of the lattice gauge fields the zero mode contribution is defined as the expectation value of the average gauge field,

$$\phi_\mu^a = \frac{1}{\Omega} \sum_x A_\mu^a(x) \quad . \quad (19)$$

The zero mode contribution is apparent in the momentum space propagators where one finds from eq. 16 for vanishing momentum

$$\tilde{D}_{\mu\mu}(p=0) = a^d \Omega \sum_a \langle (\phi_\mu^a)^2 \rangle \quad . \quad (20)$$

By taking the inverse Fourier transformation of Eq.(16) one can easily see that the zero modes give a constant contribution  $(N_z a)^{-1} \tilde{D}_{\mu\mu}(p=0)$  to the coordinate space propagator  $D_{\mu\mu}(z)$ . In fact, such a contribution does qualitatively explain the overall volume dependence of the magnetic propagators observed in our calculation. The contribution from zero momentum mode fluctuations is expected to vanish in the infinite volume limit. We thus expect that at fixed distance  $zT$  the propagators approach their asymptotic, infinite volume values from above as the lattice size is increased. This is indeed the case, as can be seen in Figure 5 where we show the 4d and 3d magnetic propagators calculated in Landau and Maximally Abelian gauges on different size lattices at  $T = 2T_c$ . As one can see from the figure the volume dependence is quite different in these two gauges. In the case of Landau gauge we observe that the magnetic propagators in coordinate space decay faster with increasing lattice size. In the Maximally Abelian gauge, however, the propagator does not exhibit any sizeable finite size dependence.



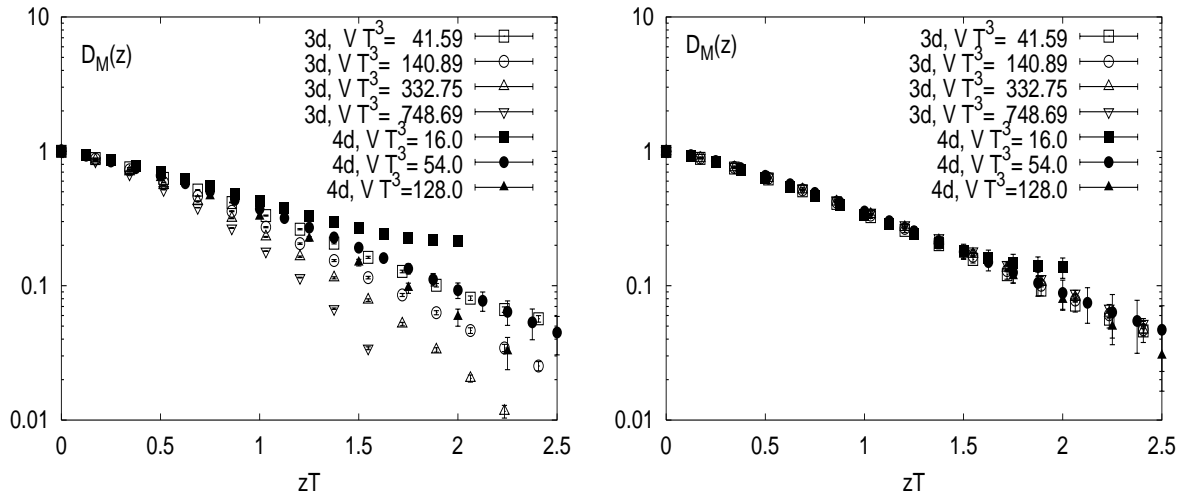


FIG. 5. Volume dependence of the magnetic propagator in coordinate space calculated in Landau (left) and Maximally Abelian (right) gauges. The propagators were normalized to 1 at  $z = 0$ . Shown are results from 3d simulations at  $\beta_3 = 8$  and 4d simulations, which are compared at similar values of the physical volume in units of  $T^3$ . These volumes correspond to lattices of size  $16^2 \times 32 \times 8$ ,  $24^2 \times 48 \times 8$  and  $16^2 \times 32 \times 4$  in 4d and to  $16^2 \times 32$ ,  $24^2 \times 48$ ,  $32^2 \times 64$  and  $48^2 \times 64$  in 3d. The  $\beta_4$  values for our 4d simulations are given in Table I.

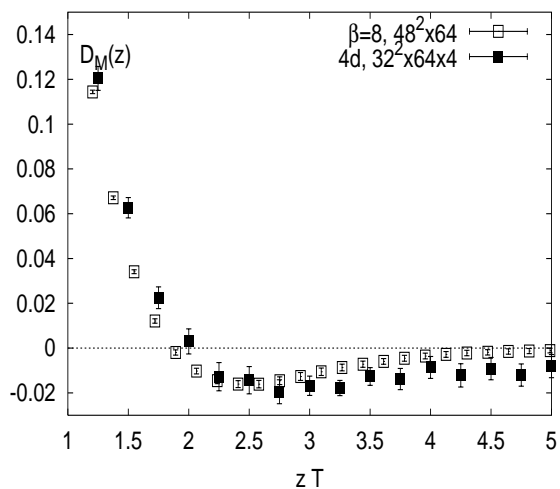


FIG. 6. Large distance behaviour of the magnetic propagator in coordinate space calculated in Landau gauge. The propagators were normalized to 1 at  $z = 0$ .

For volumes  $VT^3 \gtrsim 300$  the magnetic propagator calculated in Landau gauge becomes negative for  $zT \gtrsim 2$ . In Figure 6 we show the large distance behavior of the coordinate space propagator calculated in 4d and 3d on lattices with similar 3d lattice volume. A similar behavior of the coordinate space propagator was found in other  $\lambda$ -gauges. The propagators calculated in MAG, however, stay positive for all lattice sizes and distances accessible in our calculation, i.e. up to  $zT \sim 5$ .

As was mentioned above the magnetic propagators in the 3d adjoint Higgs model are not very sensitive to the presence of the adjoint Higgs field. This is illustrated in Figure 7 where we compare magnetic propagators in momentum space calculated in the 3d adjoint Higgs model with corresponding results obtained in the pure gauge theory at the same value of  $\beta_3$ . This also shows that the effect of the adjoint Higgs field on the magnetic propagator decreases with increasing temperature. In fact, for temperature  $T \gtrsim 10T_c$  we find no visible effect of the adjoint Higgs field on the magnetic propagators. In what follows we will therefore mainly discuss the magnetic propagators in the limit of pure gauge theory.

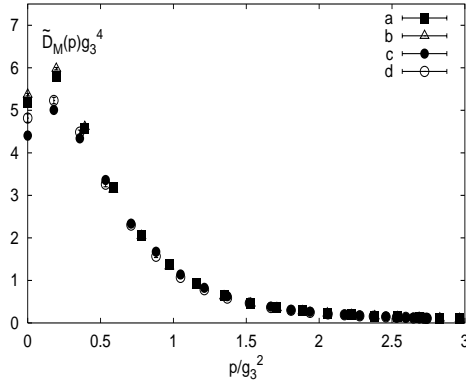


FIG. 7. Momentum space magnetic propagator obtained from 3d pure gauge theory and the adjoint Higgs model with couplings corresponding to temperatures  $2T_c$  and  $3T_c$ . Shown are the magnetic propagators in pure gauge theory at  $\beta_3 = 8$  (a), in 3d adjoint Higgs model at  $\beta_3 = 8$ ,  $x = 0.09$ ,  $h = -0.4846$  corresponding to the temperature  $3T_c$  (b), in pure gauge theory at  $\beta = 5.5$  (c) and in 3d adjoint Higgs model at  $\beta = 5.5$ ,  $x = 0.099$ ,  $h = -0.7528$  corresponding to the  $2T_c$  (d).

In Figure 8 we show the momentum space magnetic propagators in Landau gauge obtained from 3d pure gauge theory at  $\beta_3 = 5$  and  $\beta_3 = 8$ . For momenta  $p > 0.6g_3^2$  the propagators in units of  $g_3^4$  are volume and  $\beta_3$ -independent. For small momenta, however, they are strongly volume and also  $\beta_3$  dependent. One can clearly see that for large volumes the propagators reach a maximum at non-zero momentum and start decreasing with decreasing momenta. This is a direct consequence of the negative propagators in coordinate space found in Landau gauge for  $zT \gtrsim 2$ .

The volume dependence of the magnetic propagator in momentum space is strongest at  $p = 0$ . On the other hand at  $\beta_3 = 5$  one can see that the value of the propagator in the vicinity of its maximum is essentially volume independent for the three largest volumes. A similar behavior of the momentum space propagator was found in other  $\lambda$ -gauges. This is demonstrated by Figure 9. Note that although the propagator is a gauge dependent quantity the position of the peak seems to be gauge independent in the class of  $\lambda$ -gauges considered here.

The existing rigorous bound on the infrared behavior of the gluon propagator in momentum space imply that it is less singular than  $p^{-2}$  in 4d and  $p^{-1}$  in 3d [46]. It has been further argued that it is likely to vanish at zero momentum in the thermodynamic limit [47]. These considerations were also extended to the case of magnetic propagators in gauge theories at finite temperature [48]. We have analyzed this question by performing studies of the volume dependence of the zero momentum propagator. The data for  $\tilde{D}_M(0)$  are shown in Figure 10 for different  $\beta_3$  values. For  $\beta_3 = 5$  and  $\beta_3 = 8$  the data have been fitted to the ansatz

$$\tilde{D}_M(0)g_3^4 = a(Vg_3^6)^{-z} + b \quad . \quad (21)$$

We have performed fits with  $b = 0$  and  $b > 0$ . In the first case we have obtained rather large  $\chi^2$  values (typically the value of  $\chi^2/d.o.f$  was between 4 and 10) for both  $\beta_3 = 5$  and  $\beta_3 = 8$ . The three parameter fits give a reasonably good  $\chi^2$  for both  $\beta_3$  values. Using the whole range of volumes one finds  $a = 51(11), b = 2.06(15)$  and  $z = 0.34(3)$  with  $\chi^2/d.o.f. = 1.8$  for  $\beta_3 = 5$  and  $a = 52(9), b = 2.08(33)$  and  $z = 0.31(3)$  with  $\chi^2/d.o.f. = 1.8$  for  $\beta_3 = 8$ . Although the volume dependence of  $\tilde{D}_M(0)$  seems to be  $\beta_3$ -independent, the value of the exponent  $z$  as well as the value of  $\tilde{D}_M(0)$  in the infinite volume limit strongly depends on the range of volumes used in the fit. For example fitting the data on  $\tilde{D}_M(0)$  for  $\beta_3 = 5$  using lattice volumes from  $30^3$  to  $96^3$  one gets :  $a = 281(139), b = 2.52(56)$  and  $z = 0.55(5)$ . In order to firmly determine the functional form of the volume dependence of  $\tilde{D}_M(0)$  and the value  $\tilde{D}_M(0)$  in the infinite volume limit simulation on even larger lattices are necessary.

In order to confirm the infrared suppression of  $\tilde{D}_M(p)$  and the existence of a maximum in  $\tilde{D}_M(p)$  at non-zero momentum we have analyzed in more detail the interplay between infinite volume and continuum limit.

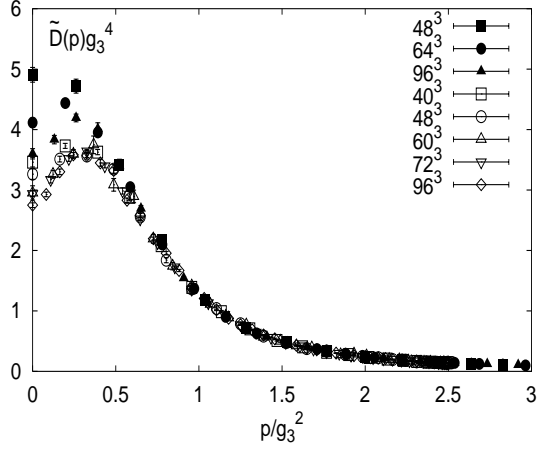


FIG. 8. The momentum space magnetic propagator at  $\beta_3 = 5$  (open symbols) and  $\beta_3 = 8$  (filled symbols) calculated in Landau gauge.

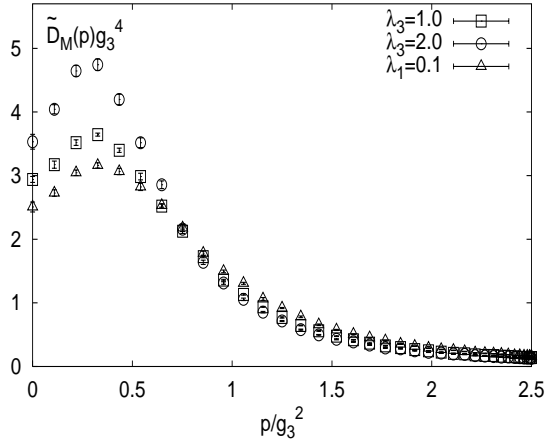


FIG. 9. The momentum space magnetic propagator at  $\beta_3 = 5$  on  $72^3$  lattice in different  $\lambda$ -gauges.

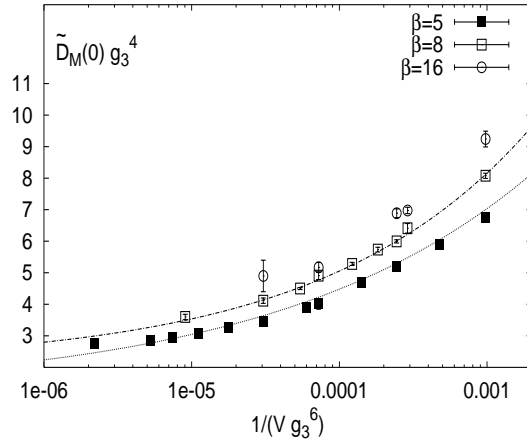


FIG. 10. Volume dependence of  $D_M(0)$  at different values of  $\beta_3$ . The lines represent fits with the ansatz given in Eq.(21).

We have seen that the propagators are infrared suppressed for large enough volumes at  $\beta_3 = 5$  and 8. However, the magnitude of the propagator at small momenta shows a clear  $\beta_3$ -dependence. Therefore, it is important to estimate the behavior of the magnetic propagator in the continuum limit. We have seen that at  $\beta_3 = 5$  the magnetic propagator on a  $60^3$  lattice is already close enough to the corresponding infinite volume limit. Therefore we have performed additional calculations of the magnetic propagators at  $\beta_3 = 6$  and on  $72^3$ . The lattice volumes  $60^3$ ,  $72^3$  and  $96^3$  at  $\beta_3 = 5, 6$  and 8 correspond to the same physical volume. Moreover, for small momenta  $p < 0.5g_3^2$ , values of the propagators at approximately same values of momenta are available. In this region of momenta we have performed an extrapolation to the continuum limit fitting data at different  $\beta_3$  with the ansatz  $a + b/\beta_3$ . The result of this analysis is summarized in Figure 11.

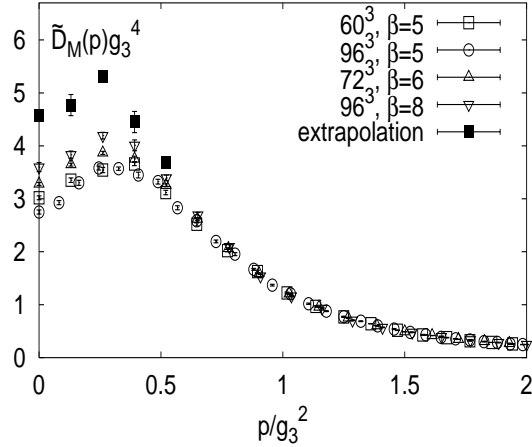


FIG. 11. The Landau magnetic propagator at different values of  $\beta_3$  and the continuum extrapolation.

As one can see from this figure the general structure of the propagator, in particular the existence of a maximum at non-zero momentum is preserved in the continuum limit, although the volume dependence of the momentum space propagator rapidly increases with decreasing momentum for  $p/g_3^2 \leq 0.5$ .

### B. The electric gluon propagator

Let us now turn to a discussion of the electric gluon propagator. The volume dependence of the electric propagator turns out to be quite different from the magnetic ones. The electric propagators show exponential decay at large distances in all gauges considered.

In Figure 12 the Landau gauge electric propagators in momentum space are shown for  $T = 2T_c$  and  $T = 9200T_c$ . In the latter case we performed the analysis only in the 3d effective theory at  $x = 0.03$ ,  $\beta = 16$  and  $h = -0.2085$ . As one can see from the figure the volume dependence of the electric propagators is indeed quite different from the volume dependence of the magnetic propagators. In particular the electric propagators show no sign of infrared suppression. For fixed lattice geometry, i.e. fixed ratio  $N/N_z$  the volume dependence of the zero mode contribution seems to approach  $V^{-1}$  as expected for the propagator of a massive particle. Moreover, the infinite volume limit is almost reached on the largest lattices used in our simulations. We find a similar volume dependence also in other gauges.

Since we are interested in extracting the screening mass from the electric propagator it is also important to address the question of volume dependence of the electric mass. In Figure 13 the local electric masses in Landau gauge are shown for different lattice volumes for  $\beta_3 = 16$ ,  $h = -0.2085$  and  $x = 0.03$ . As one can see from the figure, the value of the plateau (which in fact determines the screening mass) is essentially volume independent, although there is some volume dependence in the local masses at short distances. Thus the screening masses can be estimated even from the smallest lattice for these values of the parameters. We will use this fact in the discussion of the gauge dependence of the electric screening mass.

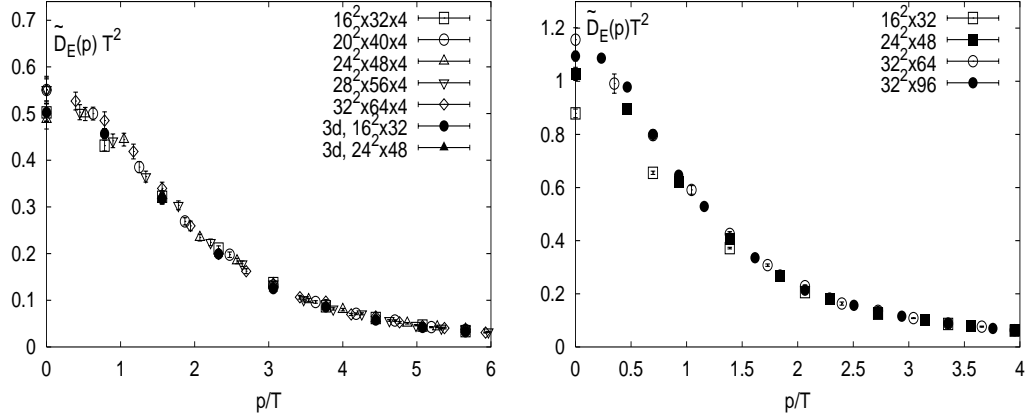


FIG. 12. The Landau gauge electric propagator in momentum space at  $2T_c$  (left) and  $T = 9200T_c$  (right).

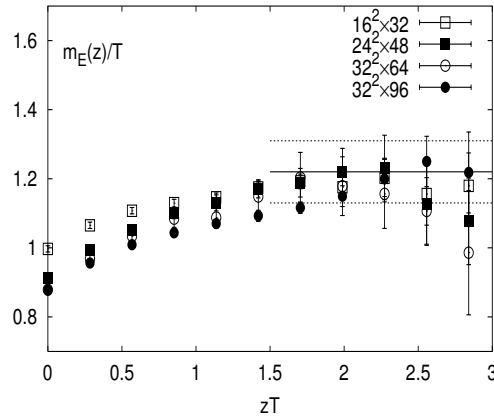


FIG. 13. Local electric masses in Landau gauge for  $\beta = 16$ ,  $h = -0.2085$  and  $x = 0.03$ . The solid line is the value of the electric mass obtained from an exponential fit of the electric propagator calculated on a  $32^2 \times 96$  lattice. The dashed lines indicate the uncertainty in its value.

Since the electric propagators show exponential decay at large distances in all gauges considered it is natural to ask whether the electric masses extracted from them are gauge independent. There is a formal proof that poles of finite temperature propagators are gauge independent to any order of perturbation theory [5]. However, as discussed in section I the Debye mass is not calculable in perturbation theory beyond leading order. Therefore it is not clear whether the arguments of Ref. [5] apply for electric screening mass. In terms of the effective 3d theory the screening of static electric fields is related to propagation of the adjoint scalar field. Since the 3d theory is confining the adjoint scalar field is not a physical state (the physical states are some bound states) and therefore there is no physical principle which guarantees its mass to be gauge invariant. Guided by the analogous problem in 3d scalar QED it was conjectured in Ref. [49] that the large distance behavior of the high temperature non-Abelian electric propagator is dominated by a branch cut singularity. Although this is different from the simple pole obtained in leading order perturbation theory this still leads to an exponential decay of the electric propagators in coordinate space with a gauge invariant screening mass. Thus it is clear that also the question of gauge (in)dependence of the electric screening mass is non-trivial in general.

We have studied the gauge dependence of the electric propagators for two sets of parameters of the 3d effective theory  $x = 0.03$ ,  $h = -0.2085$ ,  $\beta_3 = 16$  and  $x = 0.03$ ,  $h = -0.1510$ ,  $\beta_3 = 24$  both corresponding to the temperature  $T = 9200T_c$ . In this investigation lattices with spatial volume  $16^2 \times 32$ ,  $24^2 \times 48$  and  $32^2 \times 96$  were used. From studies of the Landau gauge propagators we know that electric masses for  $\beta_3 = 16$  can be reliably extracted already from  $16^2 \times 32$  lattice. We have investigated electric propagators in different gauges introduced in section II.B. For  $\beta_3 = 16$  most simulation were performed on  $16^2 \times 32$  lattice. For calculations with  $\lambda_3$  gauges we also used a  $32^2 \times 96$  lattice.

For  $\beta_3 = 24$  propagators in all gauges except the Maximally Abelian gauge were measured on  $32^2 \times 96$  lattice. Due to the large number of iterations required for fixing the Maximally Abelian gauge propagators were measured only on a  $24^2 \times 48$  lattice at  $\beta_3 = 24$ .

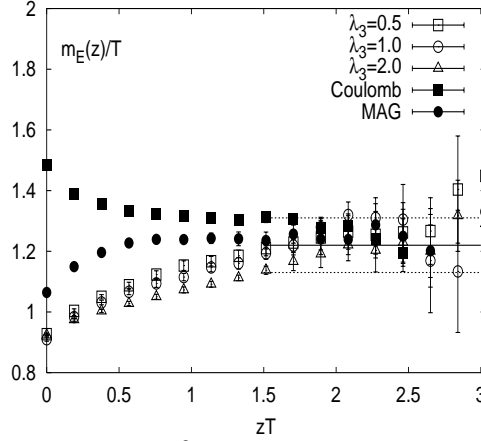


FIG. 14. The local electric masses calculated on  $32^2 \times 96$  for  $x = 0.03$ ,  $h = -0.1510$  and  $\beta_3 = 24$  in  $\lambda_3$ -gauges, in 3d Coulomb gauge ( $c_1 = 1$ ) and in Maximally Abelian gauge. The solid line is the value of the electric mass obtained from an exponential fit of the electric propagator in Landau gauge calculated on a  $32^2 \times 96$  lattice for  $\beta = 16$ ,  $h = -0.2085$  and  $x = 0.03$ . The dashed lines indicate the uncertainty in its value.

Our main results for  $\beta_3 = 24$  are summarized in Figure 14, where local electric screening masses in Coulomb, Maximally Abelian and  $\lambda_3$ - gauges are shown. As one can see from the figure local masses are strongly gauge dependent at short distances. For  $zT \gtrsim 2$  they, however approach a plateau which is gauge independent within the statistical accuracy reached in our calculation.

We also have performed simulations on a  $16^2 \times 32$  lattice for  $\beta_3 = 16$  using Coulomb gauges with  $c_1 = 0.1, 10$ , as well as  $\lambda_1$ -gauges with  $\lambda_1 = 0.1, 10$  and Maximally Abelian gauge. The corresponding results for local electric masses are shown in Figure 15. Again within statistical accuracy no gauge dependence of the plateau of the local electric masses can be observed, though the local masses have quite different  $z$ -dependence.

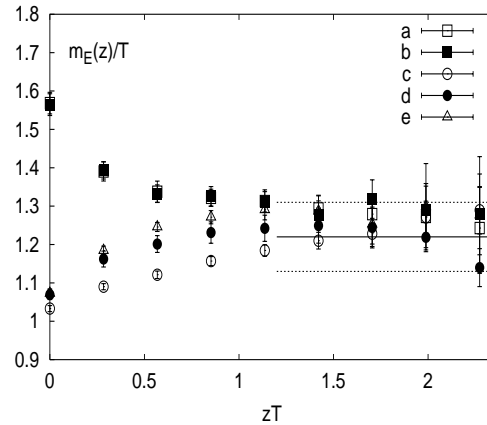


FIG. 15. The local electric masses calculated for  $x = 0.03$ ,  $h = -0.2085$  and  $\beta_3 = 16$  on  $16^2 \times 32$  lattice. Shown are the local electric masses calculated in  $c_1$  gauges for  $c_1 = 0.1$  (a) and  $c_1 = 10$  (b), in  $\lambda_1$  gauges for  $\lambda_1 = 0.1$  (c) and  $\lambda_1 = 10$  (d) and Maximally Abelian gauge (e). The solid line is the value of the electric mass obtained from an exponential fit of the electric propagator in Landau gauge calculated on a  $32^2 \times 96$  lattice  $\beta = 16$ ,  $h = -0.2085$  and  $x = 0.03$ . The dashed lines indicate the uncertainty in its value.

## IV. CONCLUSIONS

We have investigated electric and magnetic gluon propagators in the high temperature phase of SU(2) pure gauge theory in different gauges. The propagators were calculated directly in full 4d theory and also in 3d effective theory. It was shown that the effective theory can describe the electric and magnetic propagators remarkably well down to temperature  $T = 2T_c$ . We find that electric propagator can safely be extrapolated to the infinite volume limit within the statistical accuracy of our present analysis and the class of gauges considered here its long distance behaviour is gauge independent and yields a gauge independent electric screening mass which is compatible with earlier determinations.

The magnetic propagator, however, has a complicated volume and gauge dependent infrared structure which is not compatible with a simple pole mass. While it still shows a simple exponential decay at large distances in the Maximally Abelian gauge it starts getting negative for  $zT \gtrsim 2$  in a class of  $\lambda$ -gauges which includes the Landau gauge. This leads to the infrared suppression of the propagator in momentum space and is incompatible with a simple pole in the magnetic gluon propagator as it was deduced from earlier studies [8,20,21,36] which were limited to shorter distances and smaller lattices. Nonetheless, we find in all gauges that magnetic correlators are screened at large distances.

### Acknowledgements:

This work has been supported by the TMR network Finite Temperature Phase Transition in Particle Physics (EU contract no. ERBFMRX-CT-970122) and by the DFG under grant Ka 1198/4-1. Our calculations have been partially performed at the HLRS in Stuttgart and the  $(PC)^2$  in Paderborn. The work of A.C. also has been supported by FAPESP (Proj. no. 00/05047-5).

## APPENDIX

We will discuss here the procedure we followed to fix the couplings of the 3d adjoint SU(2) Higgs models. Two different approaches were proposed for fixing the parameters appearing in (2), the usual perturbative dimensional reduction [12,9] and non-perturbative matching analyzed in [8]. Here we have used both approaches.

The lattice gauge coupling  $\beta_3$  is related to the dimensionful 3d continuum gauge coupling  $g_3^2$  by the standard relation

$$\beta_3 = \frac{4}{g_3^2 a}. \quad (22)$$

This relation basically determines the lattice spacing  $a$  in terms of the dimensionful coupling  $g_3^2$ . The Higgs self-coupling and the 3d gauge couplings are related to the renormalized gauge coupling  $g(\mu)$  of SU(2) gauge theory in  $\overline{MS}$  scheme. The corresponding relations were calculated in Ref. [12] to 2-loop level.

To fix the temperature scale one needs to choose the renormalization scale  $\mu$  which fixes the temperature dependence of the 4d gauge coupling. For this we will use information on the temperature dependence of the spatial string tension. The analysis of Ref. [50] showed that the spatial string tension can be well described in terms of 3d effective theory. Furthermore it was observed that the temperature dependence of the spatial string tension of finite temperature SU(2) gauge theory can well be described by a simple formula  $0.334(14)g^2(T)T$  [51] with  $g(T)$  given by the 1-loop renormalization group relation. The string tension of the pure 3d SU(2) gauge theory was found to be  $0.335(2)g_3^2$  [52]. The string tension of the 3d adjoint SU(2) theory has been calculated in [14]. Within statistical errors it turned out to be independent of the scalar couplings and equal to the string tension of the pure SU(2) gauge theory. Based on these observations we have fitted the data on the spatial string tension from [51] using  $0.335(2)g_3^2$  with 1-loop level coupling  $g_3^2$  and the relation  $T_c = 1.06\Lambda_{\overline{MS}}$  from [21]. The fit yields  $\mu = 18.86T$ . We have also fitted the data for the spatial string tension using the 2-loop formula for  $g_3^2$  from [12]. However, it turned out that the simple 1-loop formula fits the 4d data on spatial string tension much better. Based on these observation the 3d gauge coupling  $g_3^2$  and the Higgs self-coupling were chosen according to the 1-loop version of formulas (2.13) and (2.15) from [12]

$$g_3^2 = g^2(\mu) T, \quad (23)$$

$$x = \frac{g^2(\mu)}{3\pi^2}, \quad (24)$$

with  $\mu = 18.86T$ . In Ref. [8] the parameters  $g_3^2$  and  $x$  were chosen according 2-loop formulas from [12] and  $\mu = 2\pi T$ . We have checked that differences between the present choice and that used in [8] are about 10%. In Ref. [14] the parameters of the effective theory were also calculated using the 2-loop formulas from [12], however, the 4d gauge coupling constant was determined from 1-loop formula in  $\overline{MS}$ -scheme with  $\mu \sim 7.0555$ . In Ref. [14] the screening masses extracted from gauge invariant correlators were calculated in the effective 3d theory and compared with the corresponding results from 4d simulations [18,19]. A rather good agreement between the screening masses calculated in 3d effective and full 4d theories was found. However, the 3d gauge coupling constants in [14] were considerably larger than ours which would overestimate the spatial string tension by 30%. Nevertheless this contradiction can easily be resolved by noticing that the set of parameters corresponding to  $5T_c$  in [14], namely  $x = 0.104$  and  $y = 0.242$  would roughly correspond to the temperature  $2T_c$  in our approach. Using the results from [14] for these values of  $x$  and  $y$  and the value of  $g_3^2(2T_c) = 2.89T$  we get for the two smallest screening mass the values  $m(0_+) = 2.90(3)$  and  $m(0_-) = 3.91(8)$  (for details about classification of different gauge invariant screening masses see Ref. [14]). These numbers should be compared with those obtained in 4d simulation in [19] at  $T = 2T_c$ ,  $m(0_+) = 3.06(12)$  and  $m(0_-) = 4.06(12)$ . Thus it seems that with our present choice of the parameters the effective 3d theory could describe all static quantities measured so far in lattice simulations. We also note that in the case of 2+1-dimensional gauge theory at finite temperature it has been shown that the spatial string tension and gauge invariant screening masses can be simultaneously well described by the effective 2d theory [35]. In 2+1 dimensions the situation is simplified by the fact, that the gauge coupling has no renormalization scale dependence due to superrenormalizability of the theory.

Generally we have used the non-perturbatively determined values for  $h$  [8]. However, in some cases the propagators were also calculated for values of  $h$  given by perturbative dimensional reduction. The bare Higgs mass parameter  $h$  could be related to the mass parameter  $y = m_{D0}^2/g_3^4$  of the continuum adjoint Higgs model [12]

$$h = \frac{16}{\beta_3^2}y - \frac{3.1759114(4+5x)}{\pi\beta_3} - \frac{1}{\pi^2\beta_3^2} \left( (20x - 10x^2)(\ln \frac{3}{2}\beta_3 + 0.09) + 8.7 + 11.6x \right), \quad (25)$$

with  $m_{D0}$  being the tree-level (from the point of view of the effective theory) Debye mass. At 1-loop level one has:

$$y = \frac{m_{D0}^2}{g_3^2} = \frac{2}{9\pi^2x}. \quad (26)$$

From Eqs. (25) and (26) we have calculated values of  $h$  corresponding to the 1-loop level dimensional reduction. In this case simulation were performed in the metastable brunch of the broken phase (see Ref. [12] for details).

Numerical values for the couplings of the 3d effective action used in most of our calculations are summarized in Table III together with the corresponding values of  $T/T_c$ . For other values of  $\beta_3$  used in our calculations we have calculated the coupling  $h$  from Eq. (25) using the  $y$  values from Table III.

$x$	$T/T_c$	$\beta_3$	I		II		pert	
			$h$	$y$	$h$	$y$	$h$	$y$
0.099	2.0	11	-	-	-	-	-0.3773	0.2274
0.090	2.8	16	-0.2611	0.3556	-0.2622	0.4007	-0.2700	0.2755
0.070	9.0	16	-0.2528	0.4408	-0.2490	0.5009	-0.2588	0.3470
0.050	72.1	16	-0.2365	0.5914	-0.2314	0.6721	-0.2437	0.4756
0.030	9200	16	-0.2085	0.9279	-0.2006	1.0544	-0.2181	0.7758

TABLE III . Numerical values for the coupling  $h$  and continuum mass parameter  $y = m_{D0}^2/g_3^2$  of the effective 3d theory in our simulations and the corresponding values of the temperature. I and II denote two sets of  $h$ -values taken from Ref. [8]. The last two columns give the coupling  $h$  and mass parameter  $y$  obtained from the perturbative relations Eqs. (25) and (26).

The electric propagators show exponential decay at large distances. Therefore it is possible to extract screening masses from them. The procedure of extracting the screening masses from the propagators was described in Ref. [8]. In Figure 16 we compare the electric screening masses extracted from the Landau gauge propagators in the 3d adjoint Higgs model calculated on  $32^2 \times 64$  and  $32^2 \times 96$  lattices with the corresponding results from 4d SU(2) gauge theory [21]. The parameters of the effective theory were chosen according to Table III.



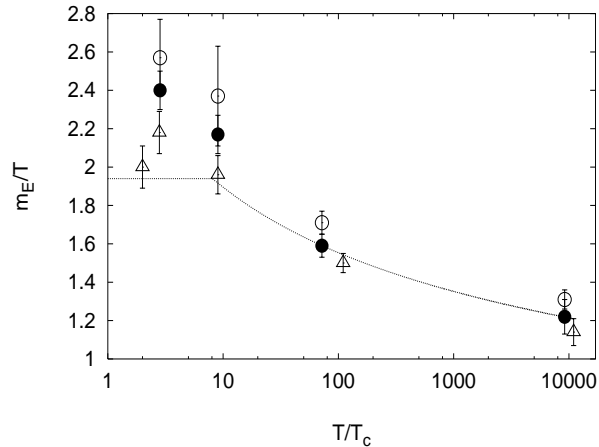


FIG. 16. The electric screening masses in units of the temperature. Shown are the electric masses  $m_E$  for the first (filled circles) and the second (open circles) set of  $h$ . The line represent the fit for the temperature dependence of the electric mass from 4d simulations. The open triangles are the values of the electric mass for  $h$  values obtained from perturbative reduction in the metastable region (the last column in Table III). Some data points at the temperature  $T \sim 70T_c$  and  $T \sim 9000T_c$  have been shifted in the temperature scale for better visibility.

As one can see from the figure the agreement between the masses obtained from 4d and 3d simulation is rather good. The electric mass shows some dependence on  $h$ . For relatively low temperatures ( $T < 50T_c$ ) the best agreement with the 4d data for the electric mass is obtained for values of  $h$  corresponding to 2-loop dimensional reduction and lying in the metastable region. This fact motivated our choice of the parameters of the effective theory at  $T = 2T_c$  in section III. For higher temperatures, however, practically no distinction can be made between the three choices of  $h$ .

Before closing the discussion on the choice of the parameters of the effective 3d theory let us compare our procedure of fixing the parameters of the effective theory with that proposed in [9]. In Ref. [9] the gauge coupling was fixed by matching the data on Polyakov loop correlators determined in lattice simulation to the corresponding value calculated in lattice perturbation theory. The resulting gauge couplings turned out to be considerably smaller than the corresponding ones used in our analysis, e.g. for  $T = 2T_c$  it gave  $g^2 = 1.43$  while our procedure gives  $g^2(2T_c) = 2.89$ . The scalar couplings were fixed according to 1-loop perturbation theory [9]. Using this procedure the authors of Ref. [9] obtained a good description of the Polyakov loop correlator in terms of the 3d effective theory, however, the spatial Wilson loop whose large distance behavior determines the spatial string tension was not well described in the reduced 3d theory. The reason for this is the fact that the value of the Polyakov loop correlator is cut-off dependent and therefore it is not very useful for extracting the renormalized coupling.

- 
- [1] D.J. Gross, R.D. Pisarski and L.G. Yaffe, Rev. Mod. Phys. **53** (1981) 43
  - [2] F. Karsch, A. Patkós and P. Petreczky, Phys. Lett **B401** (1997) 69
  - [3] J.O. Andersen, E. Braaten and M. Strickland, Phys. Rev. Lett. **83** (1999) 2139; Phys.Rev. **D 61** (2000) 014017; Phys.Rev. **D 61** (2000) 074016
  - [4] J.-P. Blaizot, E. Iancu and A. Rebhan, Phys. Rev. Lett. **83** (1999) 2906; Phys.Lett. **B470** (1999) 181
  - [5] R. Kobes, G. Kunstatter and A. Rebhan, Phys. Rev. Lett. **64** (1990) 2992; Nucl. Phys. **B355** (1991) 1
  - [6] A. Rebhan, Nucl. Phys. **B430** (1994) 319
  - [7] P. Arnold and L.G. Yaffe, Phys. Rev. **D52** (1995) 7208
  - [8] F. Karsch, M. Oevers and P. Petreczky, Phys. Lett. **B442** (1998) 291
  - [9] P. Lacock, D.E. Miller and T. Reisz, Nucl. Phys. **B369** (1992) 501
  - [10] L. Kärkkäinen, P. Lacock, B. Petersson and T.Reisz Nucl.Phys. **B395** (1993) 733
  - [11] L. Kärkkäinen P. Lacock, D.E. Miller, B. Petersson and T.Reisz, Nucl. Phys. **B418** (1994) 3
  - [12] K. Kajantie, M. Laine, K. Rummukainen and M. Shaposhnikov, Nucl. Phys. **B503** (1997) 357
  - [13] M. Laine and O. Philipsen, Phys. Lett. **B459** (1999) 259
  - [14] A. Hart and O. Philipsen, Nucl.Phys. **B572** (2000) 243

- [15] A. Hart, O.Philipsen and M. Laine, Nucl.Phys. **B586** (2000) 443
- [16] K. Kajantie, M. Laine, J. Peisa, A. Rajantie, K. Rummukainen and M. Shaposhnikov, Phys. Rev. Lett. **79** (1997) 3130
- [17] M. Laine and O. Philipsen, Nucl. Phys. **B523** (1998) 267
- [18] S. Datta and S. Gupta, Nucl. Phys. **B534** (1998) 392
- [19] S. Datta and S. Gupta, Phys.Lett. **B471** (2000) 382
- [20] U.M. Heller, F. Karsch and J. Rank, Phys. Lett. **B355** (1995) 511
- [21] U.M. Heller, F. Karsch and J. Rank, Phys. Rev. **D57** (1998) 1438
- [22] A. Cucchieri, F. Karsch and P. Petreczky, Phys.Lett. **B497** (2001) 80
- [23] C. Bernard, D. Murphy, A. Soni and K. Yee, Nucl. Phys. B (Proc. Suppl.) **17** (1990) 593
- [24] C. Bernard, A. Soni and K. Yee, Nucl. Phys. B (Proc. Suppl.) **20** (1991) 410
- [25] A. Kronfeld et al, Phys. Lett. **B198** (1987) 516
- [26] K. Amemiya and H. Suganuma, Phys.Rev. **D60** (1999) 114509
- [27] C. Curci, P. Menotti and G. Paffuti, Z. Phys. **C26** (1985) 549
- [28] T. Reisz, J. Math. Phys. **32** (1991) 515
- [29] J.E. Mandula and M. Ogilvie, Phys. Lett. **B248** (1990) 156
- [30] Ph. de Forcrand and R. Gupta, Nucl. Phys. **B** (Proc. Suppl.) **9** (1989) 516
- [31] A. Cucchieri, Nucl. Phys. **B508** (1997) 353
- [32] A. Cucchieri and F. Karsch, Nucl. Phys. B (Proc. Suppl.) **83** (2000) 357
- [33] A. Cucchieri, Phys. Rev. **D60** (1999) 034508
- [34] C. Bernard et al, Phys. Rev. **D49** (1994) 1589.
- [35] P. Bialas, A. Morel, B. Petersson, K. Petrov, T. Reisz, Nucl.Phys. **B581** (2000) 477
- [36] F. Karsch, T. Neuhaus, A. Patkós and J. Rank, Nucl. Phys. **B474** (1996) 217
- [37] G. Alexanian and V.P. Nair, Phys. Lett. **B352** (1995) 435
- [38] W. Buchmüller and O. Philipsen, Nucl. Phys. **B443** (1995) 47
- [39] F. Eberlein, Phys. Lett. **B439** (1998) 130; Nucl. Phys. **B 550** (1999) 303
- [40] D. Karabali and V.P. Nair, Phys. Lett. **B379** (1996) 141; D. Karabali, C. Kim and V.P. Nair, Nucl. Phys. **B524** (1998) 661
- [41] R. Jackiw and S.-Y. Pi, Phys. Lett. **368** (1996) 131
- [42] J. Cornwall, Phys. Rev. **D57** (1998) 3698
- [43] D.B. Leinweber, J.I. Skullerud, A.G. Williams and C. Parinello, Phys. Rev. **D58** (1998) 0315011
- [44] L. von Smekal, R. Alkofer and A. Hauck, Phys. Rev. Lett. **79** (1997) 3591 ; Ann. Phys. **267** (1998) 1
- [45] G. Damm, W. Kerler, V. K. Mitrjushkin, Phys.Lett. **B433** (1998) 88
- [46] D. Zwanziger, Nucl. Phys. **B364** (1991) 127
- [47] D. Zwanziger, Nucl. Phys. **B412** (1994) 657
- [48] I. Zahed and D. Zwanziger, Phys. Rev. **D61** (2000) 037501
- [49] J.-P. Blaizot and E. Iancu, Nucl. Phys. **B459** (1996) 559
- [50] M. Caselle and A. D'Adda, Nucl.Phys.**B427** (1994) 273
- [51] G.S. Bali, J. Fingberg, U.M. Heller, F. Karsch and K. Schilling, Phys. Rev. Lett. **71** (1993) 3059
- [52] M. Teper, Phys. Rev. **D59** (1999) 014512